Anion and Cation Effects on Olefin Adsorption on Silver and Copper Halides: Ab Initio Effective Core Potential Study of π-Complexation

Helen Y. Huang, Joel Padin, and Ralph T. Yang*

Department of Chemical Engineering, University of Michigan, Ann Arbor, Michigan 48109-2136

Received: July 2, 1998; In Final Form: November 10, 1998

An ab initio molecular orbital study using the effective core potentials (ECP) is performed to determine the anion and cation effects on the adsorption of C_2H_4 and C_3H_6 on CuX and AgX (X = F, Cl, Br, I). Compared with all-electron calculations, the ab initio ECPs require only a fraction of the computational resources with accuracy that approaches that of the all-electron calculations. The following trends of anion and cation effects were obtained for the adsorption of C_2H_4 and C_3H_6 on the metal halides: $F^- > Cl^- > Br^- > I^-$ for anions, and $Cu^+ > Ag^+$ for cations. These trends are in excellent agreement with the experimental results. In addition, the theoretical metal−olefin bond energies are in fair agreement with the experimental data. A detailed analysis of the electronic distribution is also performed using natural bond orbital (NBO) theory. The NBO results show that the d−π* back-donation is about twice that of the σ donation for the Cu^+−olefin bonds, whereas the two donations are of the same order for the Ag^+−olefin bonds. Hence, the Cu−C bonds contain more metal d than metal s character. For both metals, there is considerable electron redistribution upon olefin bonding, from the d_{z^2} orbital to the d_{yz} orbital. Such redistribution apparently enhances the d−π* back-donation.

Introduction

Adsorption by π-complexation is a most promising alternative to cryogenic distillation for olefin/paraffin separations. Cryogenic distillation has been used for these separations for over 60 years.[1] It remains to be the most energy-intensive distillation because of the close relative volatilities of olefin and paraffin. The advantage of adsorption by π-complexation is that the bonds formed between absorbent and absorbate via π-complexation are stronger than those by van der Waals forces alone, so it is possible to have high selectivity and high capacity for the component to be bound. At the same time, the bonds are still weak enough to be broken by employing simple engineering processes such as raising the temperature or decreasing the pressure of the system.

The model of π-complexation was originally proposed by Dewar[2] to explain the bonding in π-coordinated metal−olefin complexes. He described the formation of these complexes as due to the two-way donor−acceptor interactions. One is the charge donation from the filled π orbital of the ligand into the vacant s orbital of the metal and the other is the back-donation from the d orbital of the metal to the vacant π* orbital of ligand, as shown in Figure 1. In 1953, Chatt and Duncanson[3] first applied the theory of "π-coordinated metal−olefin complexes" to explain the nature of the chemical bond in platinum−olefin complexes. This classic description has since been widely used for analyzing the chemical properties of metal−ligand complexes. The study of such complexes may lead to more insight into areas such as adsorption, homogeneous and heterogeneous catalysis, surface chemistry, and organometallic chemistry.

Recently, a number of highly efficient π-complexation adsorbents have been developed in our laboratory for selective olefin adsorption. These include Ag^+-exchanged resins, monolayer $CuCl/\gamma$-Al_2O_3,[4,5] monolayer CuCl on pillared clays,[6] and monolayer $AgNO_3/SiO_2$ sorbent.[7] These sorbents, based on π-complexation, are able to selectively adsorb olefins (C_2H_4 or C_3H_6) over paraffins. The π-complexation bonds have been studied further through molecular orbital calculations.[8,9]

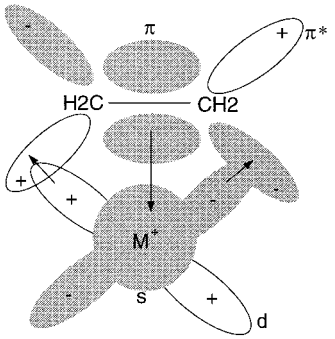

Figure 1. Schematic representation of a metal−olefin complex.

It is likely that anion as well as cation have strong effects on the ability of the sorbents to form π-complexation bonds with the olefins. The purpose of this study is to determine these effects and to employ ab initio molecular orbital theory for a basic understanding of these effects.

Experimental Section

Equilibrium isotherms were made utilizing a Micromeritics ASAP 2010. The ASAP 2010 utilizes a volumetric system to obtain adsorption isotherms. Equilibrium isotherms were measured at 25 and 0 °C to obtain isosteric heat of adsorption data. The ethylene and propylene used for this experiment were obtained from Matheson Gas (CP grade, Matheson minimum purity 99.0%). The gases were used without further purification. All of the silver and copper salts utilized in this work were obtained from Strem Chemicals. The samples were degassed

* Corresponding author. Phone: (734) 936-0771. Fax: (734) 763-0459. E-mail: yang@umich.edu.

10.1021/jp982857c CCC: $18.00
Published on Web 04/01/1999

in vacuo at 100 °C before each experiment to remove any impurities adsorbed.

Computational Details

Calculations were performed at the restricted Hartree−Fock (RHF) and density functional theory (DFT) using effective core potentials (ECP)[10−12] for Cu, Ag, and X (X = Cl, Br, I) atoms at the double-ζ-type valence basis set level, whereas Dunning's basis set (D95) was used for F, C, and H atoms. Gaussian 94 program package[13] was used for all the calculations.

Density Functional Theory (DFT). Density functional theory (DFT) was applied to analyze the metal−olefin bond features in terms of the natural bond orbital (NBO) scheme. In recent years, DFT has been recognized as a promising approach in the field of ab initio calculations. It is found that the methods originated in DFT are advantageous, since they provide an accurate description of the metal−ligand interactions without losing the simple chemical interpretation arising from a single-determinant scheme.[14] In particular, it has been found that a great improvement over the standard DFT can be achieved by a hybrid method consisting of HF and DFT, leading to the so-called self-consistent hybrid (SCH) approaches.[15] The SCH approaches are able to provide reliable geometric, thermodynamic, and spectroscopic parameters for a wide class of metal−ligand interactions, ranging from covalent bonds to weak noncovalent interactions.[16−18] The advantage of these methods is that it incorporates electron correlation at an affordable computational cost, so it is an efficient tool for studying molecular properties of large molecules such as compounds of transition metals. In this work, we selected one of the most useful SCF approaches, the B3LYP[19] approach, which is the combination of HF and Becke exchange[20] with the Lee−Yang−Parr (LYP) correlation potential.[21]

Effective Core Potentials (ECP). Applications of the all-electron ab initio molecular orbital calculations have been restricted to small molecules because the computational cost increases as N^4, where N is the number of electrons. In addition, for the heavier elements, relativistic effects must be considered, which have a significant influence on the physicochemical properties of molecules.[10] The use of effective core potentials (ECP) has been a notable success in the molecular orbital calculations involving transition metals. An excellent discussion/review on ECP studies of transition metal bonding, structure, and reactivity has been made by Gordon and Cundari.[22] ECP is simply a group of potential functions that replace the inner-shell electrons and orbitals that are normally assumed to have minor effects on the formation of chemical bonds. Calculations of the valence electrons using ECP can be carried out at a fraction of the computational cost that is required for an all-electron (AE) calculation, while the overall quality of computation does not differ much from the AE calculations.[10,11] In addition, the relativistic mass−velocity and Darwin terms, which are derived from all-electron relativistic Hartree−Fock calculations, are implicitly incorporated into the relativistic effective core potentials (RECP) for heavier elements (Z > 36).[23,24] Combined with the use of reliable basis sets, it appears to be a very powerful and economical method for dealing with molecules containing heavy transition metals. Recently, Hay and co-workers have shown that effective core potentials can be used reliably in density functional computations as well.[25] Following this approach, the LanL2DZ basis set was employed for both geometry optimization and NBO analysis in this work. The LanL2DZ basis set is a double-ζ basis set containing effective core potential representations of electrons near the nuclei for post-third-row atoms. The reliability of this basis set has been confirmed by the accuracy of calculation results compared with experimental data as well as those from a more expensive all-electron basis set.

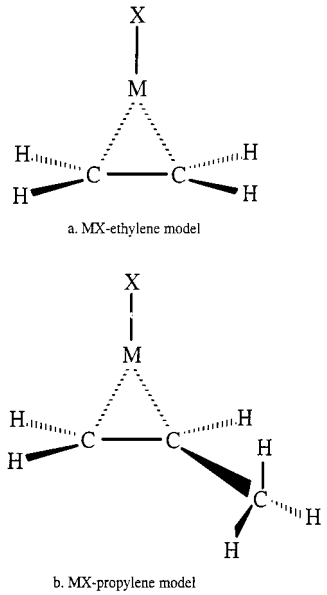

Figure 2. Theoretical models for MX−olefin complex: (a) MX−ethylene model; (b) MX−propylene model.

Geometry Optimizations and Energy of Adsorption Calculations. The restricted Hartree−Fock (RHF) theory at the LanL2DZ level basis set was used to determine the geometries and the bonding energies of C_2H_4 and C_3H_6 on AgX and CuX (X = F, Cl, Br, I). The optimized structures were then used for energy calculation and NBO analysis at the B3LYP/LanL2DZ level. The computational models used for the adsorption systems are shown in Figure 2. The models were chosen to be as simple as possible with only a single MX interacting with one unsaturated hydrocarbon. The main reason for this is to analyze the model using π-complexation theory; the same meaningful conclusions from a study with clusters would always be achieved as far as the analysis of the two-way donor−acceptor model is concerned, since the metal bears the same electronic configuration.[26] On the other hand, the purpose of this work is to study the anion (F^-, Cl^-, Br^-, I^-) and cation (Ag^+ and Cu^+) effects on the adsorption of C_2H_4 and C_3H_6 on MX, so what we are concerned with most in this study is the *trend* of the properties of the adsorption systems, while the absolute values are not as important for this study. Moreover, since the same theory and basis set were used for all the calculations, they are generally of nearly equal accuracy for all the elements, so they can reveal reliable trends as well as possible experimental inaccuracies.

The determination of bond energies of the metal−olefin bonds is important for predicting stable structures and adsorption mechanisms. In this work, the bond energies have been calculated using the optimized geometries and according to the following expression:

$$E_{ads} = E_{adsorbate} + E_{adsorbent} - E_{adsorbent-adsorbate} \qquad (1)$$

where $E_{adsorbate}$ and $E_{adsorbent}$ are the total energies of the adsorbate (C_2H_4 or C_3H_6) and the bare adsorbent (AgX or CuX), respectively, and $E_{adsorbent-adsorbate}$ is the total energy of the adsorbate/adsorbent system. A higher E_{ads} corresponds to a stronger adsorption.

Natural Bond Orbital (NBO). Information concerning atomic charge distributions is important for understanding and

TABLE 1: Fitting Parameters for C_3H_6 (Eq 2) on AgX and CuCl

	BET surface area (m^2/g)	0 °C		25 °C		
		q_0 (mmol/g)	k_p (1/atm)	q_0 (mmol/g)	k_p (1/atm)	$-\Delta H$ (kcal/mol)
AgF	10	0.102	0.185	0.092	0.065	9.0
AgCl	11	0.073	0.242	0.031	0.0118	8.4
AgBr	9	0.062	0.204	0.036	0.021	7.7
AgI	13	0.062	0.184	0.034	0.124	7.3
CuCl	8	0.091	0.330	0.034	0.026	10.0

correlation of chemical phenomena. Among the numerous schemes proposed for atomic population analysis, only that of the Mulliken[27] population analysis has been widely used. Unfortunately, Mulliken populations fail to give a useful and reliable characterization of charge distribution in many cases.[28−30] Natural population analysis (NPA) seems to be a promising alternative to conventional Mulliken population analysis. It gives a better description of the electron distribution in compounds of high ionic character, such as those containing metal atoms.[31] The NPA includes a series of calculations such as the determination of natural atomic orbitals (NAOs), natural hybrid orbitals (NHOs), natural bond orbitals (NBOs), and natural localized molecular orbitals (NLMOs). It performs population analysis and energetic analysis that pertain to localized wave function properties. It is very sensitive for calculating localized weak interactions, such as charge transfer, hydrogen bonds, and weak chemisorption. Therefore, the NBO program[32] included in Gaussian 94[13] was used for studying the electron density and charge distribution of the adsorption systems.

Results and Discussion

Experimental Results: Anion/Cation Effects and Heats of Adsorption. To determine the anion effects, equilibrium isotherms for C_3H_6 and C_2H_4 on AgX salts (where X = F, Cl, Br, I) were measured at 0 and 25 °C. The selection of these salts allowed us to maintain the cation constant while varying the anion. It also simplified the analysis due to the similarities in electron configuration of all the anions used. The equilibrium data were fitted with the Langmuir isotherm with two parameters shown below:

$$q = \frac{q_{mp} b_p p}{1 + b_p p} \tag{2}$$

where q is the amount adsorbed at pressure p, and b_p and q_{mp} are the parameters. To account for differences in surface area between the various halide salts, the isotherms were normalized by reporting the data as amount adsorbed per surface area.[33] The BET surface areas for the salts are shown in Table 1. The normalized isotherms for C_3H_6 and C_2H_4 on Ag^+ halide salts at 0 °C are reported in Figures 3 and 4, respectively. Fitting parameters for these isotherm are shown in Tables 1 and 2. Once the data were normalized, olefin molecules showed a greater affinity for the AgF salt. The corrected adsorption trend was as follows:

$$\text{AgF} > \text{AgCl} > \text{AgBr} > \text{AgI}$$

The above trend is also supported by isosteric heats of adsorption data obtained from the temperature dependence of the equilibrium isotherms. Isosteric heats of adsorption ($-\Delta H$) values for propylene on AgF, AgCl, AgBr, and AgI salts at a loading of 0.003 mmol/g were calculated at 9.0, 8.4, 7.7, and 7.3 kcal/mol. Similarly, ethylene isosteric heats of adsorption for the above salts at a loading of 0.0014 mmol/g were calculated at 7.2, 6.9, 6.0, and 5.1 kcal/mol.

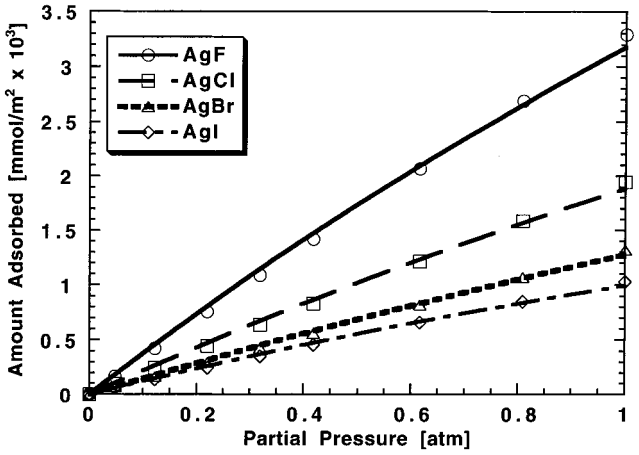

Figure 3. Normalized C_3H_6 adsorption isotherm on AgX (X = F, Cl, Br, I) salts at 0 °C.

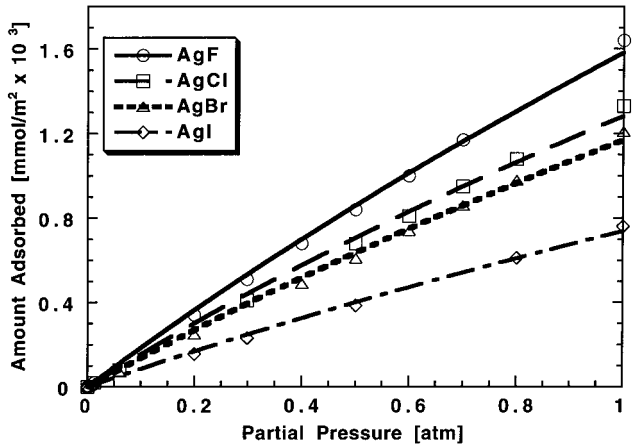

Figure 4. Normalized C_2H_4 adsorption isotherm on AgX (X = F, Cl, Br, I) salts at 0 °C.

TABLE 2: Fitting Parameters for C_2H_4 (Eq 2) on AgX and CuCl

	0 °C		25 °C		
	q_0 (mmol/g)	k_p (1/atm)	q_0 (mmol/g)	k_p (1/atm)	$-\Delta H$ (kcal/mol)
AgF	1.170	0.014	1.170	0.0035	7.2
AgCl	0.375	0.023	0.375	0.0060	6.9
AgBr	0.400	0.028	0.400	0.0085	6.0
AgI	0.380	0.019	0.038	0.0058	5.1
CuCl	0.144	19.25	0.144	4.09	8.3

To determine the cation effects, C_3H_6 and C_2H_4 equilibrium isotherms on AgCl and CuCl salts were measured at 0 and 25 °C. In this series of experiments the anion (Cl^-) was kept constant while varying the cation from Ag^+ to Cu^+. Again, the equilibrium data were fitted to the Langmuir isotherm model shown in eq 2. The fitting parameters are shown in Tables 1 and 2. The normalized isotherms for C_3H_6 and C_2H_4 on AgCl and CuCl at 0 °C are reported in Figures 5 and 6, respectively. The surface area values measured for AgCl and CuCl are shown in Table 1. From the normalized data, it can be observed that CuCl adsorbs olefins more strongly than AgCl. This observation is also supported by isosteric heat of adsorption ($-\Delta H$) data. The heats of adsorption for C_3H_6 on CuCl and AgCl at a loading of 0.003 mmol/g were calculated at 10.0 and 8.4 kcal/mol, respectively. Also supporting this trend, the heats of adsorption

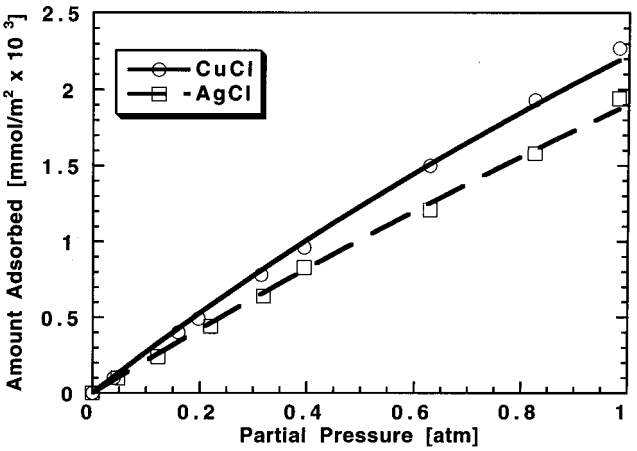

Figure 5. Normalized C_3H_6 adsorption isotherm on CuCl and AgCl salts at 0 °C.

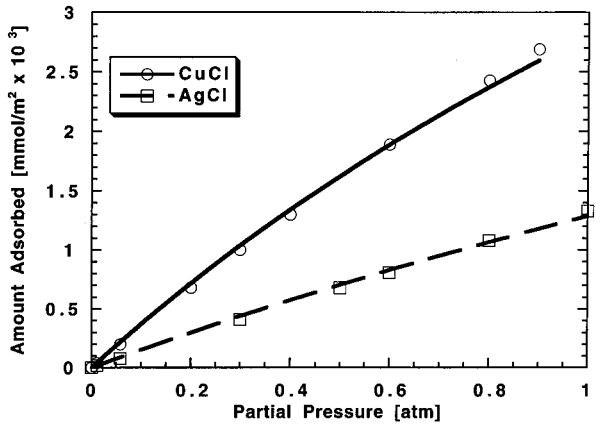

Figure 6. Normalized C_2H_4 adsorption isotherm on CuCl and AgCl salts at 0 °C.

for C_2H_4 on CuCl and AgCl at a loading of 0.0014 mmol/g were calculated at 8.3 and 6.9 kcal/mol, respectively.

In the next section, the above trends will be further explained and a mechanism describing the various cation and anion effects will be elucidated using ab initio molecular orbital calculations.

Geometries and Bond Energies: Anion Effects. The optimized geometry for free ethylene is very close to the experimental data, with C−C bond length = 1.334 Å, C−H bond length = 1.075 Å, and H−C−H angle = 116.4°. The experimental values[34] are 1.34 Å, 1.09 Å and 117.8°, respectively. The equilibrium structure found for all the MX−C_2H_4 complexes (Table 3) have the C_{2v} symmetry with M approaching the π bond along the perpendicular bisector of the C−C bond. The C−C bond midpoint is at the origin, with the C−C bond along the *y* axis and the metal atom on the *z* axis. Two equal length metal−carbon bonds were formed to give a three-membered ring with ethylene (Figure 7). Our results of optimized CuX−C_2H_4 are consistent with the study of Merchan and co-workers,[35] who also found the most stable structure of Cu^+−C_2H_4 to involve the perpendicular approach of Cu^+ to the midpoint of the C−C bond and a value of 2.322 Å obtained for the optimal distance between the Cu^+ and the ethylene plane. As shown in Table 3, our results show Cu−C distances of 2.33−2.43 Å from F to I, which are close to the literature data. The optimized Ag−C distances are about 0.3 Å longer than that of Cu−C and follow the same order, i.e., AgF−C < AgCl−C < AgBr−C < AgI−C. A comparison of the bond length of free ethylene with ethylene in the MX−C_2H_4 complexes shows that, upon adsorption, the C−C bond length increases. Also, upon

TABLE 3: Summary of Geometries and Energies of Adsorption for MX−C_2H_4 System[a]

M	X	*r*(C−C)	*r*(C−H)	*r*(M−C)	H-bend	Δ*H*	exptl Δ*H*
Cu	F	1.3489	1.0744	2.3342	2.9604	16.880	
Cu	Cl	1.3485	1.0746	2.3864	2.7394	15.743	8.3, 11.7[b]
Cu	Br	1.3478	1.0746	2.4035	2.6192	15.052	
Cu	I	1.3473	1.0747	2.4281	2.4623	14.465	
Ag	F	1.3479	1.0746	2.6176	2.7179	11.834	7.2
Ag	Cl	1.3470	1.0741	2.6367	2.6053	11.203	6.9, 10.0[c,d]
Ag	Br	1.3466	1.0745	2.6783	2.4755	10.915	6.0
Ag	I	1.3462	1.0747	2.6969	2.3848	10.397	5.1
free C_2H_4		1.3340	1.0747				

[a] The bond lengths are in angstroms, the angle of H-bend (see Figure 7) in degrees, and the energies in kcal/mol. [b] The substrate is CuCl/γ-Al_2O_3 and the experimental data for both Ag^+ and Cu^+ are taken from ref 4. [c] The substrate is Ag^+/resin. $AgSO_3C_6H_5$ is used instead of AgCl for comparison because the two anions, $SO_3C_6H_5^-$ and Cl^-, have almost the same ability for ethylene adsorption.[8]

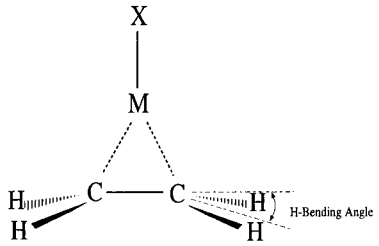

Figure 7. Optimized MX−ethylene complex.

adsorption, the four C−H bonds bend away slightly from the metal (Figure 7). This is not surprising, since other bent transition-metal−ethylene complexes are known.[36−39] The geometrical parameters also indicate that the strength of the interaction decreases from F^- to I^-. As can be seen from Table 3, the increase in the C−C bond length and the degree of H bending away from MX are in the order $F^- > Cl^- > Br^- > I^-$. The bond lengths of M−C follows the order $F^- < Cl^- < Br^- < I^-$. Since shorter bond length means stronger bonding and since the more H is bent away the stronger is the interaction between olefin and MX, the trend of the MX−C_2H_4 interactions for the same M is $F^- > Cl^- > Br^- > I^-$, which agrees with the experimental results and also with the calculated energy of adsorption.

Optimization results of free C_3H_6 and MX−C_3H_6 complexes are summarized in Table 4. The calculated geometries of free C_3H_6 are also in good agreement with experimental values,[34] with C−C double bond length of 1.335 Å and C−C single bond length of 1.517 Å and the corresponding experimental data being 1.34 and 1.50 Å, respectively. The same trend of anion effects on C_3H_6 adsorption can also be observed from an examination of the structure parameters. However, the way that C_3H_6 deforms upon adsorption is different from that of C_2H_4 because of the differences in the free molecular structures. Two metal−carbon bonds were also formed to yield a three-membered ring with the two double-bonded carbons (C1 and C2). But the two M−C bond lengths are different, with one of them shorter and the other longer than the corresponding M−C bonds with ethylene. The shorter M−C1 bond indicates a stronger MX−olefin interaction. This is consistent with the higher heats of adsorption for C_3H_6 on MX than C_2H_4 on the same MX as shown in Tables 3 and 4. The longer M−C2 bond length can be explained through the NBO analysis. The NBO population analysis shows that the electron population is higher on C1 than on C2, which means it is a better electron donor to form the π-complexation with metal. Thus, the M−C1 interaction is stronger than M−C2 interaction and the M−C1 bond length is shorter than M−C2.

TABLE 4: Summary of Geometries and Energies of Adsorption for $MX-C_3H_6$ System[a]

M	X	*r*(C1−C2)	*r*(C2−C3)	*r*(M−C1)	*r*(M−C2)	ΔH	exptl ΔH
Cu	F	1.3512	1.5106	2.2862	2.4061	19.753	
Cu	Cl	1.3505	1.5102	2.3255	2.4654	18.855	10.0, 14.2[b]
Cu	Br	1.3502	1.5100	2.3388	2.4837	18.164	
Cu	I	1.3497	1.5099	2.3543	2.5014	17.578	
Ag	F	1.3499	1.5106	2.5644	2.7021	14.314	9.0
Ag	Cl	1.3493	1.5103	2.6006	2.7443	13.967	8.4
Ag	Br	1.3489	1.5102	2.6125	2.7623	13.557	7.7
Ag	I	1.3484	1.5100	2.6280	2.7838	13.034	7.3
free C_3H_6		1.3346	1.5172				

[a] The bond lengths are in angstroms and the energies in kcal/mol. C1 and C2 are double-bonded carbons, and C3 is the third carbon atom. [b] The substrate is $CuCl/\gamma$-Al_2O_3, and the experimental data for both Ag^+ and Cu^+ are taken from ref 4.

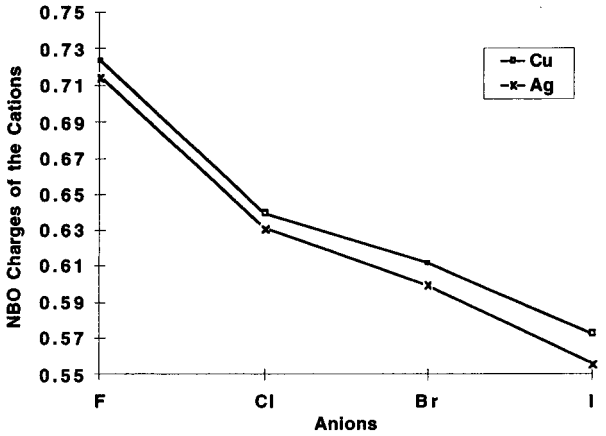

Figure 8. NBO atomic charges for CuX and AgX.

The changes in structure parameters of olefins and the formation of M−C bonds can be explained through π-complexation theory as discussed earlier. In the interaction of olefin with a transition metal, donation and back-donation processes take place. The first consequence of the donation and back-donation processes is the weakening of the C−C bond strength (donation of π-bonding electron from olefin to the s orbital of metal and back-donation of d electron from metal to the antibonding π orbitals both have the effect of weakening the C−C bonding). A stronger deformation of the molecule indicates a stronger adsorption of olefin on MX.

The trend of anion effects on the adsorption of olefin can be interpreted in terms of the different electronegativities of the anions, i.e., following the order F > Cl > Br > I. An element with a stronger electronegativity would "attract" more electrons from the metal bonded to it, while metals with more positive charges will be better acceptors to form π bonds with the olefin.[8] The NBO charge analysis of MX shown in Figure 8 manifests this trend. From this plot, it is obvious that the positive charge on M drops dramatically from MF to MI, which corresponds to the stronger interaction of MF with olefins than MI with olefins.

Cation Effects. The effects of cation on olefin adsorption are also seen in Tables 3 and 4. With the same anions, $CuX-C_2H_4$ and $CuX-C_3H_6$ show longer C−C bond, shorter M−C bond, and stronger H bending than the corresponding $AgX-C_2H_4$ and $AgX-C_3H_6$. These are consequences of stronger interactions of CuX with olefins than that of AgX with olefins. Results from NBO analysis can help explain this trend. As shown in Figure 8, the amount of positive charge on CuX and AgX is Cu > Ag. As stated above, metals with more positive charge will be better acceptors to form π-complexation with olefins. With a more positive charge than Ag^+, Cu^+ attracts more electrons from the olefin. This means a stronger σ donation from olefin to the vacant s orbital of Cu^+. Thus, the bond distance between M and C is shorter for Cu. Shorter M−C distance at the same time leads to more overlap of the π^* orbital of the olefin with the d orbitals of metal, which means a stronger d−π^* back-donation between M and C. These two factors result in the above geometric differences between CuX and AgX with both C_2H_4 and C_3H_6.

Bond Energies. The energies of adsorption calculated using eq 1 are also shown in Tables 3 and 4. A good comparison between the theoretical values and experimental values is seen (Tables 3 and 4). The anion and cation effects on the adsorption of olefin are correctly predicted, i.e., $F^- > Cl^- > Br^- > I^-$ and $Cu^+ > Ag^+$. The agreement between the experimental and theoretical values is quite satisfactory, taking into account the limitations of theory. These include the inaccuracies associated with the quantum chemical method and errors caused by the finite size of the model used for the solid surface.[40] Also, the theoretical difference between $MX-C_2H_4$ and $MX-C_3H_6$ is consistent with the π bonding being stronger in propylene than in ethylene.

To compare results between ECP and the higher level all-electron basis sets, we have used basis set 6-31+G for F and Cl (it is not available for Br, I, and Ag), and even higher heats of adsorption than that from ECP were obtained. This was probably caused by the overemphasis of the electron interactions that resulted in higher energies. It is recommended that the same basis set and method should be used for comparison of different molecules. The only available all-electron basis sets for Ag, I, and Br are STO-3G and 3-21G. These have been used in the work, but the results were not satisfactory.

Nature of the Bonding. The nature of the metal−olefin bond can be better understood by analyzing the NBO results. The main feature of the bonding can be seen from the population changes in the vacant outer-shell s orbital of the metal and those in the d shells of the metal upon adsorption.[41] The NBO analysis, summarized in Tables 5 and 6, is generally in line with the traditional picture of Dewar[2] and Duncanson and Chatt[3] for metal−olefin complexation; i.e., it is dominated by the donation and back-donation contributions. An examination of the tables shows that in all cases the M−C interaction is a dative bond, i.e., donation of electron charges from the π orbital of olefin to the vacant s orbital of metal and, simultaneously, back-donation of electron charges from the d orbitals of M to the π^* orbital of olefin (Figure 1). This can be interpreted in more detail as follows. When the olefin molecule approaches M^+, some electronic charge is transferred from the C=C π orbital to the valence s orbital of M^+; at the same time, electrons in the filled d orbitals of metal are transferred to the symmetry-matched π^* orbital of olefin. It can be seen from Tables 5 and 6 that upon adsorption, the electron occupancies of the valence s orbitals of Cu and Ag always increase, whereas the total occupancy of their 4d or 5d orbitals always decreases. Obviously, this is

TABLE 5: Summary of the NBO Analysis of π-Complexation between MX and C_2H_4[a]

	C → M interaction (σ donation) q_1	M → C interaction (d−π* back-donation) q_2	net change $q_1 + q_2$
$CuF-C_2H_4$	0.047	−0.089	−0.042
$CuCl-C_2H_4$	0.052	−0.080	−0.028
$CuBr-C_2H_4$	0.042	−0.077	−0.035
$CuI-C_2H_4$	0.030	−0.072	−0.042
$AgF-C_2H_4$	0.081	−0.073	+0.008
$AgCl-C_2H_4$	0.058	−0.053	+0.004
$AgBr-C_2H_4$	0.047	−0.049	−0.002
$AgI-C_2H_4$	0.032	−0.044	−0.011

[a] q_1 is the amount of electron population increase on valence s orbitals of the metal, and q_2 is the total amount of electron population decrease on valence d orbitals of the metal.

TABLE 6: Summary of the NBO Analysis of π-Complexation between MX and C_3H_6[a]

	C → M interaction (σ donation) q_1	M → C interaction (d−π* back-donation) q_2	net change $q_1 + q_2$
$CuF-C_3H_6$	0.046	−0.080	−0.034
$CuCl-C_3H_6$	0.051	−0.085	−0.034
$CuBr-C_3H_6$	0.040	−0.071	−0.031
$CuI-C_3H_6$	0.028	−0.067	−0.039
$AgF-C_3H_6$	0.081	−0.071	+0.010
$AgCl-C_3H_6$	0.060	−0.054	+0.006
$AgBr-C_3H_6$	0.046	−0.047	−0.001
$AgI-C_3H_6$	0.031	−0.043	−0.012

[a] q_1 is the amount of electron population increase on valence s orbitals of the metal, and q_2 is the total amount of electron population decrease on valence d orbitals of the metal.

caused by the donation and back-donation of electrons between metal and olefin as stated above.

A comparison of the electron population changes in the s and d orbitals of M before and after adsorption shows that for the CuX−olefin complexes, the overall charge transfer is back-donation. The amount of back-donation is about double the amount of σ donation. This indicates that the Cu−C bonds contain more metal d than metal s character and that the strength of the covalent bonds depends mainly on the overlap of the metal d orbitals with the C hybrid orbitals.[42] For the AgX−olefin complexes, quite differently, the back-donation is almost equal to the σ donation, which means the σ donation and back-donation play equally important roles in the bonding of Ag−C. A comparison of the net changes of the electron occupation on the two different metals before and after adsorption shows greater net electron occupation changes on Cu than that on Ag upon olefin adsorption. As discussed in the literature,[43] the amount of change indicates the extent of interaction. This is consistent with the conclusion that CuX has a stronger interaction with olefin than AgX.

To gain further insight into the bonding between metal and olefin, we list in Table 7 the changes in electron populations of the five d orbitals of Cu and Ag upon ethylene adsorption. As we can see clearly from the table, the interactions of the five d orbitals with ethylene are skewed. Orbitals d_{xy}, d_{xz}, and $d_{x^2-y^2}$ have almost no contribution to the overlap with the π* orbitals of the olefin, since there is no or little change in their electron population upon ethylene adsorption. The main depopulation occurs in the d_{yz} and d_{z^2} orbitals. This is because the three inactive orbitals (d_{xy}, d_{xz}, and $d_{x^2-y^2}$) are pointing in directions perpendicular to that of d_{yz} (in which plane the three-member ring C−C−M lies); there is little chance for them to overlap with the d_{yz} orbital. The depopulation in the d_{yz} orbital can be explained easily with the classic picture of π-complexation, shown in Figure 1. However, the smaller amount of population decrease in the d_{z^2} orbitals is not expected. This phenomenon can be understood with the concept of "electron redistribution" that we proposed previously.[9] As shown in Figure 9, the dumbbell-and-doughnut-shaped d_{z^2} orbitals are in the vicinity of the spatial directions of the d_{yz} orbitals and can overlap to some extent with the d_{yz} orbitals. This result indicates that there is a considerable electron redistribution between the d_{yz} and d_{z^2} orbitals during the metal−olefin bonding. Obviously, electron redistribution from the d_{z^2} to the d_{yz} orbitals helped enhance the d−π* back-donation.

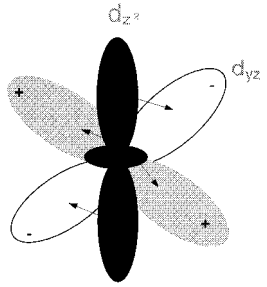

Figure 9. Schematic representation of electron redistribution from metal d_{z^2} to d_{yz}.

TABLE 7: Electron Population Changes on d Orbitals of Cu and Ag after C_2H_4 Adsorption

	d_{xy}	d_{xz}	d_{yz}	$d_{x^2-y^2}$	d_{z^2}
$CuF-C_2H_4$	0	0	−0.0823	−0.0015	−0.0051
$CuCl-C_2H_4$	0	0	−0.0604	−0.0012	−0.0187
$CuBr-C_2H_4$	0	0	−0.0558	−0.0011	−0.0197
$CuI-C_2H_4$	0	0	−0.0505	−0.0010	−0.0202
$AgF-C_2H_4$	0	0	−0.0387	0	−0.0342
$AgCl-C_2H_4$	0	0	−0.0370	0	−0.0310
$AgBr-C_2H_4$	0	0	−0.0264	0	−0.0229
$AgI-C_2H_4$	0	0	−0.0239	0	−0.0201

Conclusion

In this study, the anion and cation effects on the adsorption of olefins (C_2H_4 and C_3H_6) on MX (M = Cu, Ag and X = F, Cl, Br, I) were studied by the ab initio effective core potential studies of the MX−olefin complexes. The ab initio calculations correctly predicted the trend of the effects, which are $F^- > Cl^- > Br^- > I^-$ and $Cu^+ > Ag^+$. The calculated results of geometries and bond energies of the complexes are in good agreement with reported literature data and experimental results. The metal−olefin bond energies are in good agreement with the experimental heats of adsorption results. The bonding features of metal−olefin were studied by NBO analysis. The NBO results showed that the d−π* back-donation is a main contribution to the metal−olefin bonding, with Cu more so than Ag. Significant electron redistribution from the d_{z^2} to the d_{yz} orbital is observed for both metals. The redistribution is greater for Ag−olefin than for Cu−olefin. The redistribution is caused by the spatial matching between these two d orbitals, with d_{yz} lying in the plane of the three-member C−C−M ring.

Acknowledgment. This work was supported by the National Science Foundation Grant CTS-9520328.

References and Notes

(1) Keller, G. E.; Marcinkowsky, A. E.; Verma, S. K.; Williamson, K. D. *Separation and Purification Technology*; Li, N. N., Calo, J. M., Eds; Marcel Dekker: New York, 1992; p 59.

(2) Dewar, M. J. S. *Bull. Soc. Chim. Fr.* **1951**, *18*, C71.

(3) Chatt, J.; Duncanson, L. A. *J. Chem. Soc.* **1953**, 2939.
(4) Yang, R. T.; Kikkinides, E. S. *AIChE J.* **1995**, *41*, 509.
(5) Wu, Z.; Han, S. S.; Cho, S. H.; Kim, J. N.; Chue, K. T.; Yang, R. T. *Ind. Eng. Chem. Res.* **1997**, *36*, 2749.
(6) Cheng, L. S.; Yang, R. T. *Adsorption* **1995**, *1*, 61.
(7) Rege, S. U.; Padin, J.; Yang, R. T. *AIChE J.* **1998**, *44*, 799.
(8) Chen, J. P.; Yang, R. T. *Langmuir* **1995**, *11*, 3450.
(9) Chen, N.; Yang, R. T. *Ind. Eng. Chem. Res.* **1996**, *35*, 4020.
(10) Hay, P. J.; Wadt, W. R. *J. Chem. Phys.* **1985**, *82*, 270.
(11) Wadt, W. R.; Hay, P. J. *J. Chem. Phys.* **1985**, *82*, 284.
(12) Hay, P. J.; Wadt, W. R. *J. Chem. Phys.* **1985**, *82*, 299.
(13) Frisch, M. J.; Trucks, G. W.; Schlegel, H. B.; Gill, P. M. W.; Johnson, B. G.; Robs, M. A.; Cheeseman, J. R.; Keith, T.; Petersson, G. A.; Montgomery, J. A.; Raghavachari, K.; Al-Laham, M. A.; Zakrzewski, V. G.; Ortiz, J. V.; Foresman, J. B.; Peng, C. Y.; Ayala, P. Y.; Chen, W.; Wong, M. W.; Andres, J. L.; Replogle, E. S.; Gomperts, R.; Martin, R. L.; Fox, D. J.; Binkley, J. S.; DeFrees, D. J.; Baker, J.; Stewart, J. P.; Head-Gordon, M.; Gonzalez, C.; Pople, J. A. *Gaussian 94*, revision B.3; Gaussian, Inc.: Pittsburgh, PA, 1995.
(14) Ziegler, T. *Chem. Rev.* **1991**, *91*, 651.
(15) Becke, A. D. *J. Chem. Phys.* **1993**, *98*, 1372.
(16) Ricca, A.; Bauschlicher, C. W. *J. Phys. Chem.* **1994**, *98*, 12899.
(17) Barone, V.; Adamo, C. *J. Phys. Chem.* **1996**, *100*, 335.
(18) Halthausen, M. C.; Heinemann, C.; Cornhl, H. H.; Koch, W.; Schwarz, H. *J. Chem. Phys.* **1995**, *102*, 4931.
(19) Becke, A. D. *J. Chem. Phys.* **1993**, *98*, 5648.
(20) Becke, A. D. *Phys. Rev.* **1988**, *B38*, 3098.
(21) Lee, C.; Yang, W.; Parr, R. G. *Phys. Rev.* **1988**, *B37*, 785.
(22) Gordon, M. S.; Cundari, T. R. *Coord. Chem. Rev.* **1996**, *147*, 87.
(23) Lee, Y. S.; Ermler, W. C.; Pitzer, K. S. *J. Chem. Phys.* **1977**, *67*, 5861.
(24) Kahn, L. R.; Hay, P. J.; Cowan, R. D. *J. Chem. Phys.* **1978**, *68*, 2386.
(25) Russo, T. V.; Martin, R. L.; Hay, P. J. *J. Phys. Chem.* **1995**, *99*, 17085.
(26) Miralles-Sabater, J.; Merchan, M.; Nebot-Gil, I.; Viruela-Marin, P. M. *J. Phys. Chem.* **1988**, *92*, 4853.
(27) Mulliken, R. S.; Ermler, W. C. *Diatomic Molecules: Results of Ab Initio Calculations*; Academic Press: New York, 1977; p 33.
(28) De Profit, F.; Marin, J. M. L.; Geerling, P. *Chem. Phys. Lett.* **1996**, *250*, 393.
(29) Luthi, H. P.; Ammeter, J. H.; Almlof, J.; Faegri, K. *J. Chem. Phys* **1982**, *77*, 2002.
(30) Collins, B.; Streitwieser, A. *J. Comput. Chem.* **1980**, *1*, 81.
(31) Reed, A. E.; Weinstock, R. B.; Weinhold, F. *J. Chem. Phys.* **1985**, *83* (2), 735.
(32) Glendening, E. D.; Reed, A. E.; Carpenter, J. E.; Weinhold, F. *NBO*, version 3.1; 1995.
(33) Padin, J.; Yang, R. T. *Ind. Eng. Chem. Res.* **1997**, *36*, 4224.
(34) Hehre, W. J.; Radom, L.; Schleyer, P. V. R.; Pople, J. A. *Ab Initio Molecular Orbital Theory*; Wiley: New York, 1986.
(35) Merchan, M.; Gonzalez-Luque, R.; Nebot-Gil, I.; Tomas, F. *Chem. Phys. Lett.* **1984**, *112*, 412.
(36) Basch, H.; Newton, M. D.; Moskowitz, J. W. *J. Chem. Phys.* **1978**, *69*, 584.
(37) Ozin, G. A.; Power, W. J.; Upton, T. H.; Goddard, W. A., III. *J. Am. Chem. Soc.* **1978**, *100*, 4750.
(38) Garcia-Prieto, J.; Novaro, O. *Mol. Phys.* **1980**, *41*, 205.
(39) Hay, P. J. *J. Am. Chem. Soc.* **1981**, *103*, 1390.
(40) Sauer, J. *Chem. Rev.* **1989**, *89*, 199.
(41) Nicolas, G.; Spiegelmann, F. *J. Am. Chem. Soc.* **1990**, *112*, 5410.
(42) Sodupe, M.; Bauschlicher, C. W., Jr. *J. Phys. Chem.* **1991**, *95*, 8640.
(43) Yang, R. T.; Chen, Y. D.; Peck, J. D.; Chen, N. *Ind. Eng. Chem. Res.* **1996**, *35*, 3093.